American Mineralogist, Volume 79, pages 526–535, 1994

The two-dimensional pattern of metamorphic fluid flow at Mary Kathleen, Australia: Fluid focusing, transverse dispersion, and implications for modeling fluid flow

Ian Cartwright

Victorian Institute of Earth and Planetary Sciences, Department of Earth Sciences, Monash University, Clayton, Victoria 3168, Australia

Abstract

The pattern of resetting of $\delta^{18}O$ values in layered Corella calc-silicate rocks adjacent to a scapolitized metadolerite dike at Timberu in the Mary Kathleen fold belt illustrates some of the complexities of two-dimensional metamorphic fluid flow. Fluids flowing from the dike ($\delta^{18}O$ = 9–10‰) into the calc-silicate rocks lowered calcite $\delta^{18}O$ values from 19–20‰ to as low as 10.2‰. Time-integrated advective fluid fluxes varied from 0.72 to >8.1 m^3/m^2 over a 4.5-m lateral distance, and there are two distinct channels of higher fluid flux. If the duration of fluid flow was similar across the outcrop, intrinsic permeabilities varied laterally by at least an order of magnitude. Fluid flow was largely focused across lithological layering, with rare excursions parallel to layering, suggesting that flow was probably hosted within microfractures and that the variable permeabilities resulted from variations in microfracture density. The sides of the channels show gradational $\delta^{18}O$ vs. distance profiles that are of similar width (up to 1 m) to those at the isotopic front (~1.2 m), indicating that the coefficients of transverse and longitudinal dispersion are of similar orders of magnitude. Localities in other terrains probably show similar complex patterns of isotopic resetting that in two dimensions correspond to the predictions of the advective-dispersive transport models, but which are difficult to interpret using a one-dimensional analysis. Transverse dispersion during channeled fluid flow will potentially reset O-isotope ratios adjacent to the channels and cause decoupling of geochemical parameters during advective and dispersive transport.

Introduction

Fluids have long been recognized as important agents of both contact and regional metamorphism. If present in sufficient volumes, fluids may control the stability of mineral assemblages, transport heat, cause metasomatism, affect the rheology of the crust, and thus influence deformation. Hence, documenting the patterns and mechanisms of crustal fluid flow is critical to our understanding of metamorphic processes. Fluids in metamorphic terrains may originate from devolatilization reactions, from igneous crystallization, or possibly from outside the terrain (e.g., from the surface or the mantle). Fluid flow through metamorphic rocks is probably channeled or focused at scales ranging from a few centimeters to kilometers. Fluid focusing on a centimeter to meter scale may result from variations in reaction-enhanced permeability (Rumble and Spear, 1983) or, if fluid flow is through microcracks that open up as a result of fluid overpressure (Etheridge et al., 1983; Yardley and Lloyd, 1989), variations in microcrack density.

Recent advances in the modeling of crustal fluid flow have involved application of the advective-dispersive transport equations that are commonly used in hydrogeology (e.g., Bear, 1972; deMarsily, 1986) to metamorphic environments (e.g., Bickle and McKenzie, 1987; Blattner and Lassey, 1989; Ganor et al., 1989; Harris and Bickle, 1989; Bickle and Baker, 1990; Cartwright and Valley, 1991; Bowman and Willett, 1991; Ferry and Dipple, 1992; Dipple and Ferry, 1992; Bickle, 1992; Nabelek et al., 1992; Cartwright and Weaver, 1993; Léger and Ferry, 1993; Davis and Ferry, 1993; Bowman et al., 1994). Many of these studies use the resetting of $\delta^{18}O$ values to quantify parameters such as time-integrated advective and dispersive fluid fluxes, the duration of fluid flow, intrinsic permeabilities, and the direction of fluid flow. Yet, despite the success of this approach, patterns of isotopic resetting in metasomatic rocks from many terrains do not conform well to the predictions of one-dimensional advective-dispersive transport models (e.g., Cartwright and Weaver, 1993), suggesting that fluid flow is often more complicated than is accounted for by the models. Additionally, although many terrains preserve evidence for metamorphic fluid-rock interaction, the detailed patterns and mechanisms of fluid flow are often poorly constrained.

Here, the meter-scale two-dimensional pattern of fluid flow during metamorphism in the Mary Kathleen fold belt is examined, and the degree of fluid channeling, transverse dispersion, and variations in intrinsic permeabilities are characterized. In particular this study shows that, although fluid flow on the decimeter to meter scale

0003–004X/94/0506–0526$02.00

is complex, it still largely conforms to the predictions of advection-dispersion transport models.

Geology of the Mary Kathleen fold belt

The geology of the Mary Kathleen fold belt is discussed in detail by Oliver et al. (1990, 1991, 1992), and Holcombe et al. (1991), and only a few details are given here. The Mary Kathleen fold belt is part of the Proterozoic Mount Isa inlier of Queensland, Australia, and consists of metasiltstones, metaquartzites, calc-silicate rocks, and marbles of the Corella Formation; metavolcanics and metasiltstones of the Argylla Formation; and numerous intrusive gabbroic and granitic bodies. U-Pb zircon ages from metavolcanics indicate that the Argylla and Corella sediments were deposited between 1780 and 1760 Ma (Page, 1983b). Extensive suites of granites and gabbros were emplaced soon after deposition of the sediments at 1760–1730 Ma (U-Pb zircon ages: Page, 1983b), accompanied by contact metamorphism at pressures of ~200 MPa with temperatures of up to 600 °C (Oliver et al., 1991; Cartwright and Oliver, 1992). The formation of skarns around the granites and the scapolitization of many dolerite dikes occurred during contact metamorphism. The area subsequently underwent low-pressure amphibolite-facies regional metamorphism, with peak temperatures and pressures of 550–650 °C and 300–400 MPa estimated from a variety of mineral thermometers and phase equilibria (Oliver et al., 1991). D2 deformation during the peak of metamorphism produced a series of tight, upright, north- or northwest-oriented folds that largely control the current outcrop pattern (Fig. 1). U-Pb mineral and whole rock ages (Page, 1983a, 1983b) and Rb-Sr whole rock ages (Page, 1978) indicate that the regional metamorphism was at ~1550 Ma. Fluid infiltration during regional metamorphism was often focused, either through dilational zones that opened up as a result of heterogeneous strain or along shear zones.

Timberu sample suite

Seventy-nine samples of Corella calc-silicate rocks and seven samples of a concordant scapolitized dolerate dike were collected from a single well-exposed outcrop, 4.5 × 4.5 m, near Timberu station (Figs. 1, 2). The contact between the calc-silicate rocks and the metadolerite and the layering within the calc-silicate rocks dip steeply west (Fig. 2a). The presence of scapolite in the dolerite indicates that fluid-rock interaction had occurred at this locality. Samples were collected from seven layers in the calc-silicate rock that are slightly raised (5–10 cm) with respect to adjacent layers; some additional samples were collected between the main layers. Sample position was measured using a tape measure, and measurement errors are probably no greater than ±5 cm. Fluid flow at Timberu probably occurred during the contact metamorphic event because the scapolization of dolerites in the Mary Kathleen fold belt generally occurred at that time (although metasomatism during the regional metamorphism cannot totally be discounted, e.g., Oliver et al., 1990, 1991). Timberu lies ~2 km from the Burstall granite (Fig. 1), and the metasomatism at this locality may have been part of the extensive fluid flow system that accompanied the intrusion of this body at 1730–1740 Ma (Cartwright and Oliver, 1992). The outcrop represents a section that, prior to D2 folding, would have been nearly vertical through the upper contact of the dike. In common with similar rock types throughout the Mary Kathleen fold belt, the calc-silicate rocks at Timberu contain hornblende + scapolite + calcite + quartz ± biotite assemblages that were stable during regional metamorphism (Oliver et al., 1992). Calc-silicate rocks directly adjacent to the dike contain centimeter-sized hornblende aggregates, which probably replace clinopyroxene and which were probably formed by fluid flow out of the dike into the calc-silicate rocks. The formation of scapolite and clinopyroxene suggests that fluid infiltration at this outcrop occurred at elevated temperatures (~500–600 °C: Oliver et al., 1990). The observation that the zones of hornblende segregations vary in width from 1 to 20 cm (Fig. 2) was used as a guide to sampling.

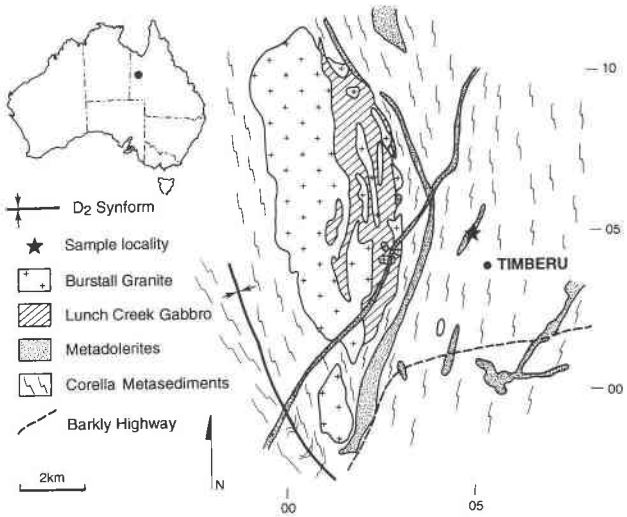

Fig. 1. Generalized geological map of part of the Mary Kathleen fold belt (after Oliver et al., 1990, 1992). Lines indicate trend of layering in the Corella calc-silicate rocks, which generally strikes north with steep dips as a result of D2 folding. Metasomatism at the Timberu locality may be associated with the intrusion of the Burstall granite at 1730–1740 Ma or be part of the 1550-Ma regional metamorphism. Numbers indicate grid references on the 1:25000-scale Marraba sheet (published by the Bureau of Mineral Resources, Canberra, Australia).

Analytical techniques

Stable isotope ratios were measured at Monash University. Silicates were analyzed following Clayton and Mayeda (1963) using ClF_3 as the reagent. CO_2 was extracted from carbonates by dissolution in H_3PO_4 (McCrea, 1950) at 25 °C for 2 h; the relatively short extraction time minimized any contribution of CO_2 from scapolite. Sample sizes were generally sufficient to yield >100 μmol of CO_2, and isotopic ratios were measured on Finnigan

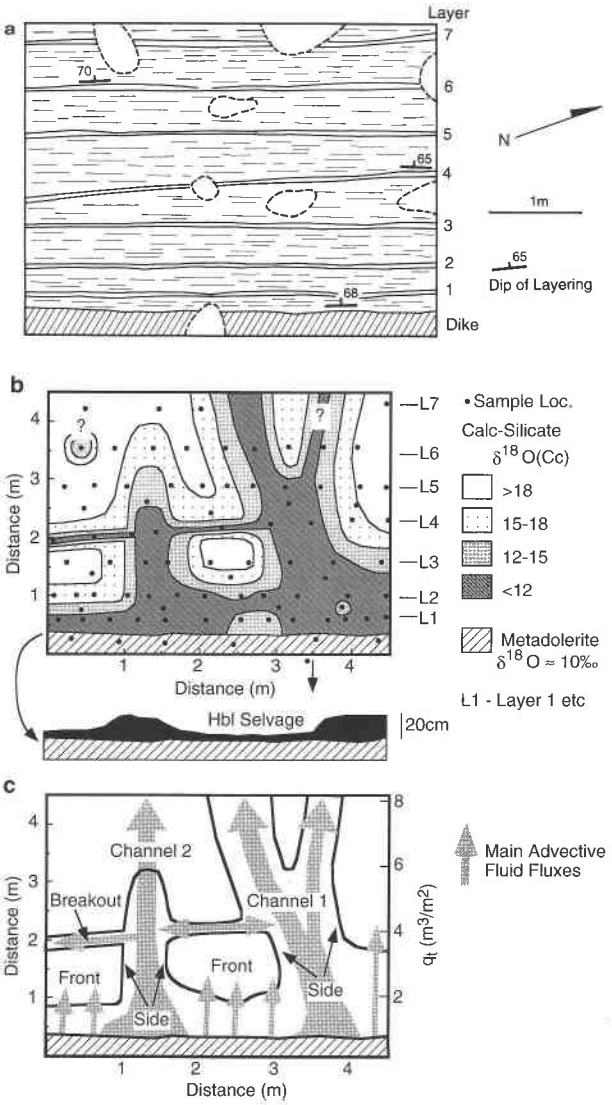

Fig. 2. (**a**) Sketch map of Timberu locality showing the main layers sampled and the orientation of the layering. (**b**) Map of $\delta^{18}O$ values at Timberu locality. The $\delta^{18}O$ (Cc) values of the calc-silicate rocks range from 19.8 to 10.2‰, whereas $\delta^{18}O$ (WR) values of the scapolitized dolerite are 9.1–10.2‰; 12, 15, and 18‰ isopleths in the calc-silicate rocks are shown. There are two distinct zones of lower $\delta^{18}O$ values extending into the calc-silicate rocks that have gradational lateral margins; the front of one of these zones is also gradational. The main layers that were used for sampling are indicated by L1–L7. L4 has low $\delta^{18}O$ values along most of its length. The detail represents observations at the contact between the dike and the calc-silicate rocks (as seen in map view), showing that the width of hornblende aggregates correlates with the two low-$\delta^{18}O$ zones. (**c**) Interpretation of $\delta^{18}O$ values using the 15‰ isopleth. The zones of low-$\delta^{18}O$ values are interpreted as channels of high fluid flux. Fluid flow was mainly across the strike, with a layer-parallel excursion along layer 4. Time-integrated fluid fluxes (q_t) were calculated from Eq. 2 for the 15‰ isopleth. Arrows show main advective fluid fluxes.

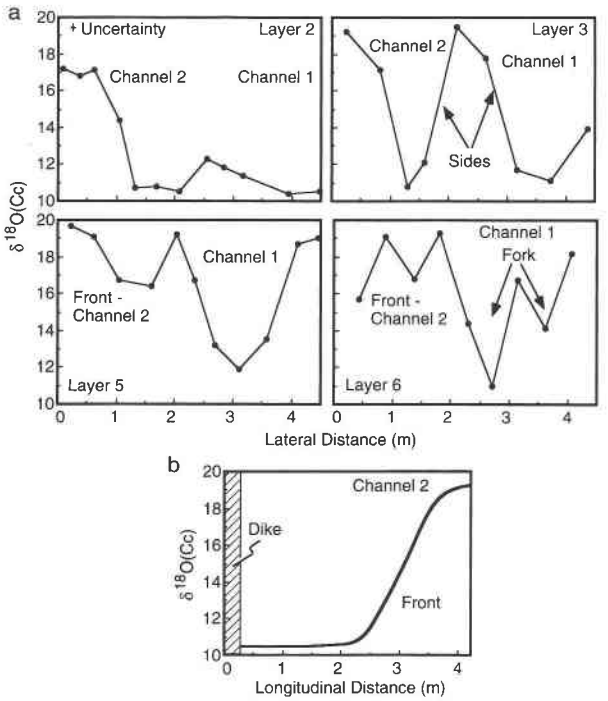

Fig. 3. Transverse and longitudinal $\delta^{18}O$ (Cc) vs. distance profiles from Fig. 1a. (**a**) The channels have gradational sides that probably result from transverse dispersion. (**b**) The front of channel 2 has a profile that is similar to those predicted by advective-dispersive transport models (e.g., Fig. 5). The estimated uncertainty is ±5 cm and ±0.2‰.

MAT Delta-E and 252 mass spectrometers. Values of $\delta^{18}O$ and $\delta^{13}C$ are reported relative to V-SMOW and PDB, respectively. Standards were analyzed at the same time as the samples reported here: NCSU quartz yielded $\delta^{18}O = 11.61 \pm 0.17$‰ ($n = 3$), and laboratory calcite CS1 yielded $\delta^{18}O = 19.87 \pm 0.09$ and $\delta^{13}C = -0.51 \pm 0.08$‰ ($n = 13$); these values are within accepted limits.

Two-dimensional fluid flow pattern

The stable isotope geochemistry of the calc-silicate rocks and metadolerite dike are summarized in Table 1 and Figures 2–4. The calc-silicate rocks have calcite (Cc) $\delta^{18}O$ values that range from 10.2 to up to 19.8‰, whereas $\delta^{13}C$ (Cc) values vary between −1.2 and 0.4‰. The higher $\delta^{18}O$ values are similar to those recorded from calc-silicate rocks elsewhere within the Mary Kathleen fold belt (Oliver et al., 1990), whereas the lower $\delta^{18}O$ values are in approximate isotopic equilibrium with the scapolitized dike ($\delta^{18}O$ = 9.1–10.2‰). Figure 2b shows the spatial pattern of $\delta^{18}O$ values with 12, 15, and 18‰ isopleths in the calc-silicate rocks. The 15‰ isopleth represents a $\delta^{18}O$ value that is midway between unreset calc-silicate rock and the scapolitized dike; such midpoint values are often used to define the position of advective fronts (Fig. 5). The 12 and 18‰ isopleths are used here to define the bounds of fully reset and unreset $\delta^{18}O$ values. The lack of distinct trends between $\delta^{13}C$ (Cc) and $\delta^{18}O$ (Cc) or be-

TABLE 1. Location, calcite content, and stable isotope geochemistry of calc-silicate rocks and metadolerite dike samples from Mary Kathleen

Sample	Position* X	Position* Y	Layer**	Wt% Cc	Calcite $\delta^{18}O$	Calcite $\delta^{13}C$	WR $\delta^{18}O$
Calc-silicate rocks							
92-MK-S1	0.13	0.59	1	22.1	10.7	0.1	
92-MK-S2	0.45	0.59	1	18.2	11.2	−0.2	
92-MK-S3	0.81	0.60	1	17.3	10.5	−0.8	
92-MK-S4	1.17	0.60	1	22.3	10.4	−0.6	
92-MK-S5	1.54	0.60	1	17.6	10.2	0.1	
92-MK-S6	2.08	0.60	1	19.3	10.8	−0.3	
92-MK-S7	2.54	0.60	1	23.2	13.6	0.0	
92-MK-S8	2.91	0.60	1	22.1	12.3	−0.8	
92-MK-S9	3.20	0.60	1	18.6	10.7	−0.9	
92-MK-S10	3.68	0.60	1	19.2	10.3	−0.2	
92-MK-S11	3.91	0.61	1	17.6	11.2	0.1	
92-MK-S12	4.19	0.61	1	18.5	10.7	−0.4	
92-MK-S13	4.50	0.61	1	22.3	10.4	0.3	
92-MK-S14	0.09	1.00	2	21.3	17.2	0.2	
92-MK-S15	0.37	1.01	2	18.7	16.8	−0.8	
92-MK-S16	0.61	1.01	2	16.9	17.1	0.0	
92-MK-S17	1.04	1.01	2	16.5	14.4	−0.6	
92-MK-S18	1.32	1.01	2	18.7	10.7	−0.4	
92-MK-S19	1.69	1.01	2	17.9	10.8	0.2	
92-MK-S20	2.07	1.01	2	17.9	10.5	−0.3	
92-MK-S21	2.54	1.01	2	21.5	12.3	−0.1	
92-MK-S22	2.83	1.01	2	22.3	11.8	−0.2	
92-MK-S23	3.27	1.02	2	17.6	11.4	−0.5	
92-MK-S24	3.95	1.02	2	18.7	10.4	−0.5	
92-MK-S25	4.47	1.02	2	19.3	10.5	−0.1	
92-MK-S26	0.44	0.75	2–1	14.2	13.4	0.0	
92-MK-S27	1.51	0.79	2–1	18.5	10.4	−0.8	
92-MK-S28	3.04	0.81	2–1	19.0	10.7	−0.3	
92-MK-S29	3.86	0.81	2–1	15.9	15.7	−0.1	
92-MK-S30	0.25	1.59	3	18.5	19.2	−0.5	
92-MK-S31	0.83	1.59	3	17.9	17.1	−0.2	
92-MK-S32	1.30	1.59	3	19.2	10.8	0.1	
92-MK-S33	1.58	1.58	3	17.6	12.1	−1.2	
92-MK-S34	2.14	1.58	3	21.3	19.5	−0.3	
92-MK-S35	2.64	1.57	3	22.1	17.8	−0.5	
92-MK-S36	3.17	1.57	3	17.0	11.7	0.4	
92-MK-S37	3.74	1.57	3	16.5	11.1	−0.2	
92-MK-S38	4.38	1.57	3	22.0	13.9	−0.1	
92-MK-S39	0.58	1.38	3–2	21.3	18.8	0.0	
92-MK-S40	2.40	1.31	3–2	19.8	15.8	−0.2	
92-MK-S41	3.65	1.32	3–2	21.3	10.8	−0.1	
92-MK-S42	0.07	1.94	4	15.6	11.1	0.1	
92-MK-S43	0.61	2.03	4	17.2	10.7	−0.2	
92-MK-S44	1.11	2.07	4	16.3	10.5	−0.4	
92-MK-S45	1.41	2.10	4	18.2	10.7	0.1	
92-MK-S46	2.28	2.17	4	17.9	11.2	−0.6	
92-MK-S47	2.92	2.21	4	15.0	11.0	−0.9	
92-MK-S48	3.47	2.27	4	14.8	11.7	−0.4	
92-MK-S49	4.00	2.30	4	17.2	16.5	−0.7	
92-MK-S50	4.48	2.30	4	18.9	19.4	−0.3	
92-MK-S51	0.22	2.87	5	21.3	19.7	0.0	
92-MK-S52	0.61	2.90	5	22.5	19.1	0.2	
92-MK-S53	1.04	2.90	5	17.8	16.7	−0.2	
92-MK-S54	1.61	2.90	5	15.9	16.4	0.2	
92-MK-S55	2.04	2.90	5	16.8	19.2	−0.3	
92-MK-S56	2.35	2.90	5	18.3	16.7	−0.8	
92-MK-S57	2.69	2.90	5	17.9	13.2	−0.6	
92-MK-S58	3.10	2.88	5	17.4	11.9	−0.7	
92-MK-S59	3.57	2.88	5	25.1	13.5	0.1	
92-MK-S60	4.10	2.88	5	18.2	18.7	0.0	
92-MK-S61	4.45	2.88	5	17.4	19.0	−0.2	
92-MK-S62	0.47	2.50	5–4	15.9	19.3	−0.2	
92-MK-S63	1.31	2.61	5–4	13.8	12.4	−0.3	
92-MK-S64	2.15	2.44	5–4	17.2	16.9	−0.7	
92-MK-S65	3.16	2.58	5–4	17.3	10.7	−0.5	
92-MK-S66	4.05	2.57	5–4	17.9	17.1	−0.4	
92-MK-S67	0.43	3.53	6	18.9	15.7	−0.8	
92-MK-S68	0.88	3.53	6	21.3	19.1	−0.9	
92-MK-S69	1.38	3.53	6	15.2	16.8	−0.2	
92-MK-S70	1.81	3.54	6	19.3	19.3	−0.6	
92-MK-S71	2.31	3.54	6	25.0	14.4	−0.7	
92-MK-S72	2.71	3.54	6	20.3	11.0	−0.1	
92-MK-S73	3.15	3.55	6	18.7	16.7	0.2	
92-MK-S74	3.61	3.55	6	17.9	14.1	−0.8	
92-MK-S75	4.07	3.55	6	17.6	18.2	−0.3	
92-MK-S76	0.48	4.21	7	18.5	17.2	−0.2	
92-MK-S77	1.45	4.21	7	18.4	19.1	−0.8	
92-MK-S78	2.00	4.21	7	17.0	17.2	−0.1	
92-MK-S79	4.45	4.30	7	15.1	19.8	−0.3	
Dike							
92-MK-D1	0.26	0.30					10.2
92-MK-D2	0.89	0.18					9.5
92-MK-D3	1.50	0.20					9.7
92-MK-D4	2.45	0.12					9.6
92-MK-D5	3.54	0.29					9.4
92-MK-D6	4.37	0.24					9.5
92-MK-D7†	—	—					9.1

* Coordinates on Fig. 2a.

** Layers on Fig. 2a; 2–1, for example, indicates a sample between layers 1 and 2.

† Sample collected ~5 m from the boundary between the dike and the calc-silicate rocks.

tween $\delta^{13}C$ (Cc) and weight percent calcite (Fig. 4) suggests that isotopic fractionation due to devolatilization was limited (Valley, 1986), indicating that infiltration of H_2O-rich fluids was probably the dominant process in resetting the isotopic ratios at Timberu. These conclusions are consistent with the findings of Oliver et al. (1990) that scapolitization of the metadolerites involved fluids of $XH_2O > 0.75$.

The pattern of isotopic resetting at Timberu suggests that fluids flowed out of the dike into the calc-silicate rocks. The scapolitized dike at Timberu has higher $\delta^{18}O$ values than unaltered dolerites elsewhere in the Mary Kathleen fold belt (typically 6–7‰: Oliver et al., 1990), and fluids derived from the Burstall granite ($\delta^{18}O$ = 8–9‰: Cartwright and Oliver, 1992) may have caused the isotopic resetting of the dike and calc-silicate rocks. The interpretation of the two-dimensional pattern of fluid flow (Fig. 2c) shows several features. (1) There are two main channels marked by zones of reset $\delta^{18}O$ values extending into the calc-silicate rocks from the dike. These channels broadly correspond to the zones where the hornblende aggregates are widest (Fig. 2b). (2) The sides of the channels preserve gradational $\delta^{18}O$ vs. distance profiles (Fig. 3a). (3) The front of channel 2 also has a gradational $\delta^{18}O$-distance profile (Fig. 3b); the front of channel 1 is not seen. (4) Fluid flow was dominantly across the layering, although a layer-parallel breakout zone exists along layer 4. Since not all layers were sampled, other breakout zones may also exist. (5) Channel 1 bifurcates around an island.

It is clear from Figure 2 that there is no single characteristic distance over which O isotope ratios have been reset. Furthermore, a suite of samples from Timberu that did not come from a line parallel to the channels would show a $\delta^{18}O$ vs. distance pattern that would be difficult to reconcile with one-dimensional models of fluid flow.

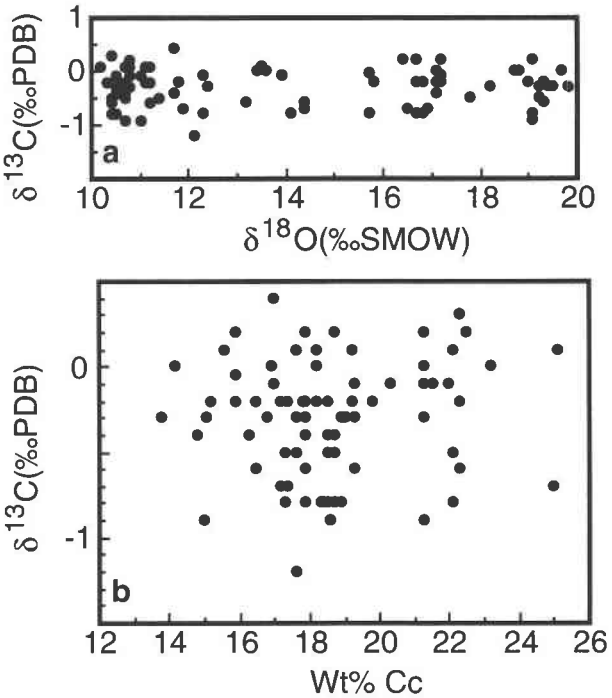

Fig. 4. (a) The $\delta^{18}O$ (Cc) vs. $\delta^{13}C$ (Cc). (b) The $\delta^{13}C$ (Cc) vs. calcite weight percent. The lack of coupled trends between these parameters suggests that fluid infiltration was the dominant process of isotopic resetting in the Timberu calc-silicate rocks (cf. Valley, 1986).

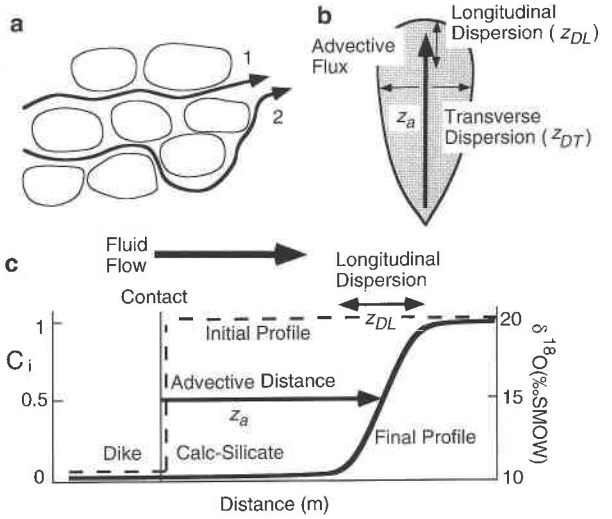

Fig. 5. Summary of aspects of the advective-dispersive transport models. (a) Differences in length between flow paths 1 and 2 may result in kinematic dispersion. (b) Longitudinal and transverse dispersion from an advective plume (after deMarsily, 1986) (c) Predicted geochemical profiles resulting from isothermal fluid transport across a contact that represents an initial geochemical discontinuity; $\delta^{18}O$ values pertain to this study. In large flow systems the width of the isotopic front is small relative to the distance of advective transport; z_a, z_{DL}, z_{DT} are the distances of advective, longitudinal dispersive, and transverse dispersive transport (see text).

Quantification of flow parameters

Fluid flow is modeled at the conditions of contact metamorphism at Mary Kathleen (~550 °C at 200 MPa), as scapolitization of many of the dolerites probably occurred at this time. However, the results of modeling fluid flow at regional metamorphic conditions (550–650 °C at 300–400 MPa) would not be significantly different and do not alter the interpretations. Overall, this type of modeling probably yields order of magnitude estimates of fluid flow parameters.

Advective-dispersive transport

The change in the concentration of chemical component i in a fluid (C_i) with time (t) during advective and dispersive transport within a porous medium is given by

$$\phi\left(\frac{\partial C_i}{\partial t}\right) = -\nabla\cdot(C_i v) + D_e\nabla^2(C_i) + R_i \qquad (1)$$

(e.g., deMarsily, 1986; Bickle and McKenzie, 1987) where ϕ is porosity, v is the Darcy fluid flux, D_e is the effective net dispersion coefficient of i in the fluid and the matrix [$D_e = (1 - \phi)D_s + \phi D_f$, where D_f and D_s are the dispersion coefficients of i in the fluid and rock, respectively], and R_i is the rate of production or consumption of component i by a reaction. During fluid flow, geochemical discontinuities are propagated in the direction of the flow by advection, and dispersion broadens the discontinuities (Fig. 5). There are two components of dispersion: (1) molecular diffusion, and (2) kinematic dispersion that results from fluid flow along paths of varying tortuosity (Fig. 5a). Mathematically, diffusion and kinematic dispersion may be modeled using the same equations, and their coefficients are additive (Bear, 1972). Two types of dispersion are addressed in this study: (1) longitudinal dispersion that acts in the direction of fluid flow, and (2) transverse dispersion that results from lateral spreading of a plume of high fluid flux (Fig. 5b).

Most studies that use O isotope ratios to model metamorphic fluid flow make assumptions and simplifications, as discussed in detail by Bickle and McKenzie (1987), Ganor et al. (1989), Bickle and Baker (1990), Cartwright and Valley (1991), Ferry and Dipple (1992), Dipple and Ferry (1992), Cartwright and Weaver (1993), and Cartwright and Oliver (unpublished manuscript). In common with those studies, the following assumptions are made here. (1) Diffusion coefficients of O within minerals are sufficiently low (10^{-16}–10^{-24} m²/s at 500–800 °C: Cole and Ohmoto, 1986) that transport through the solid matrix is insignificant; hence $D_e \approx \phi D_f$. (2) The rate of fluid-rock isotopic equilibration was sufficiently rapid that local isotopic equilibrium was maintained throughout the fluid flow episode. (3) The major cause of isotopic resetting is exchange with the infiltrating fluid. The lack of coupled $\delta^{18}O$ vs. $\delta^{13}C$ or $\delta^{18}O$ vs. weight percent calcite trends (Fig. 4) implies that isotopic resetting due to devolatilization was limited (Valley, 1986).

TABLE 2. Summary of modeling results

Parameter	Value*	Channel 2**
Time-integrated fluid flux (q_t)	0.72–>8.1 m^3/m^2	5.8 m^3/m^2
Time-integrated longitudinal dispersive flux ($D_{eL}t$)		0.18 m^2
Time-integrated transverse dispersive flux ($D_{eT}t$)	0.03–0.12 m^2	
Duration of fluid flow (t)		1.2×10^{10} to 1.2×10^{13} s (380–380 000 yr)
Fluid flux (v)		5×10^{-10} to 5×10^{-13} m^3/m^2s
Intrinsic permeability (K_e)		10^{-17}–10^{-21} m^2

* Value calculated for outcrop as a whole.
** Value calculated for channel 2 in Fig. 2.

Time-integrated advective fluxes

Time-integrated advective fluid fluxes (q_t) are given by

$$q_t = z_a K_e \tag{2}$$

(Bickle and McKenzie, 1987), where z_a is the distance parallel to the flow direction over which resetting by advection has occurred (Fig. 5), and K_e is the effective rock-fluid partition coefficient (Bickle and McKenzie, 1987). For fluids of $XH_2O = 0.75$–1.0 at 200 MPa and 550 °C, $K_e \approx 1.8$ for O_2 (Cartwright and Valley, 1991). The distance that the midpoint of the isotopic front (marked by the 15‰ isopleth) has migrated is ~0.4 to >4.5 m, with the front of channel 2 being at 3.2 m. From Equation 2, these distances yield time-integrated fluid fluxes of 0.72 to >8.1 m^3/m^2 with a flux of 5.8 m^3/m^2 for channel 2 (Table 2, Fig. 2).

Longitudinal and transverse dispersion

The distance parallel to the flow direction that the front is broadened by longitudinal dispersion (z_{DL}: Fig. 5) is given by

$$C_{i(z_{DL},t)} = \frac{1}{2}\mathrm{erfc}\left[\frac{z_{DL}}{2\sqrt{D_{eL} \cdot t/K_e}}\right] \tag{3}$$

(Crank, 1975), where D_{eL} is the effective longitudinal dispersion coefficient and erfc is the complementary error function. A similar equation relates the width of the channel side (z_{DT}) to the effective transverse dispersion coefficient D_{eT}. For channel 2, z_{DL} is ~1.2 m, and the widths of the channel sides suggest that $z_{DT} = 0.5$–1.0 m (Figs. 2, 3). The product $D_{eL}t$ represents the time-integrated longitudinal dispersive flux (Ganor et al., 1989; Cartwright and Valley, 1991). Unfortunately, there is far too little data to calculate $D_{eL}t$ values precisely by least-squares fitting (cf. Ganor et al., 1989; Bickle and Baker, 1990; Cartwright and Valley, 1991). However, at $C_i = 0.25$, $z_{DL}/2\sqrt{D_{eL}t/K_e} = 0.48$ (Crank, 1975), and for the front of channel 2, $C_i = 0.25$ ($\delta^{18}O \approx 12.5$‰) occurs at a distance of 0.3 m, yielding $D_{eL}t \approx 0.18$ m^2 (note that the distance measured here is that between the inflection point and the 12.5‰ value, not the total distance to the 12.5‰ value; Fig. 3). A similar approach yields estimates for $D_{eT}t$ of 0.03–0.12 m^2. These values are similar to estimates of time-integrated dispersive fluxes for resetting of O isotopes over similar distances at localities where a least-squares fitting approach could be adopted (Ganor et al., 1989; Cartwright and Valley, 1991). On the assumption that longitudinal and transverse dispersion operated for similar periods, these data suggest that values of D_{eL} are slightly larger than those of D_{eT}. As discussed below, these differences are possibly the result of lateral variations in intrinsic permeability.

Relative contributions of diffusion and kinematic dispersion

In hydrogeological systems the relative contributions of kinematic dispersion and diffusion to longitudinal dispersion are governed by a grain-scale Peclet number (P_e):

$$P_e = \frac{(v/\phi)l}{D_f} \tag{4}$$

(Bear, 1972, Fig. 10.4.1; deMarsily, 1986, Fig. 10.5), where l is a characteristic length of the medium (e.g., the grain diameter). The grain-scale Peclet number in Equation 4 is analogous (but not identical) to the Peclet number used to describe the relative contributions of advection and net dispersion in metamorphic fluid flow systems (e.g., Bickle and McKenzie, 1987). For the range of fluid fluxes (v) commonly proposed for metamorphic fluid infiltration (10^{-10}–10^{-14} $m^3/m^2/s$: Bickle and Baker, 1990; Dipple and Ferry, 1992; Cartwright and Weaver, 1993; Cartwright and Oliver, unpublished manuscript; Table 2), a value of D_f of 10^{-8} m^2/s (e.g., Bickle and McKenzie, 1987; Coghlin, 1990), metamorphic porosities of 10^{-3}–10^{-6} (Wood and Walther, 1986; Bickle and Baker, 1990; Cartwright and Valley, 1991), and a grain diameter of 0.001 m, $P_e = 10$–10^{-6}. Dispersion in hydrological systems with such low grain-scale Peclet numbers is dominated by molecular diffusion (Bear, 1972; deMarsily, 1986). If this is the case for metamorphic systems, the spreading of isotopic fronts parallel to the direction of fluid flow would be dominated by molecular diffusion. This conclusion is critically dependent on the assumed fluid velocities because kinematic dispersion is a function of fluid velocity. In some fluid flow systems, fluxes are possibly much higher, and kinematic dispersion will probably be more significant. For example, Bowman et al. (1994) estimated fluid fluxes of $\sim 3 \times 10^{-5}$ $m^3/m^2/s$ for fluid flow at Alta, Utah. Using this flux rate and the same values for the other parameters in Equation 4 yields $P_e \approx 3 \times 10^3$ to 3

$\times 10^6$. Comparison with the data of Bear (1972, Fig. 10.4.1; and deMarsily, 1986, Fig. 10.5) indicates that in this case kinematic dispersion would probably be a very important process (as proposed by Bowman et al., 1994). The conclusion that molecular diffusion dominated dispersion at Timberu is somewhat tentative and depends on the applicability of the data from hydrologic systems to midcrustal flow systems. The relative contributions of diffusion and kinematic dispersion to the transverse dispersive flux are much harder to estimate. However, if, as is common in hydrologic systems, coefficients of transverse kinematic dispersion are generally of the same order as or lower than those of longitudinal kinematic dispersion (Bear, 1972; deMarsily, 1986), it is likely that diffusion is also the main component of transverse dispersion.

Duration of fluid flow and intrinsic permeabilities

If diffusion is the dominant component of longitudinal dispersion, it is possible to estimate the time required to form the profiles. For porosities of 10^{-3}–10^{-6} and a value of D_f of 10^{-8} m^2/s, $D_{eL} = 10^{-11}$–10^{-14} m^2/s and, as $D_{eL}t = 1.8$ m^2, $t = 1.2 \times 10^{10}$ to 1.2×10^{13} s (380–380 000 yr) for fluid-hosted diffusion in channel 2 (Table 2). These values are similar to the estimated periods of diffusion and advection in other metamorphic terrains (e.g., Labotka et al., 1988; Ganor et al., 1989; Bickle and Baker, 1990; Cartwright and Valley, 1991). As diffusion and advection operated over the same period, these times and the time-integrated fluid flux of 5.8 m^3/m^2 yield average fluid fluxes of 5×10^{-10} to 5×10^{-13} m^3/m^2/s for channel 2 (Table 2), which are again within the range of those estimated for other metamorphic terrains.

Fluid fluxes are related to intrinsic permeability by Darcy's Law:

$$v = \frac{-K_\phi}{\eta}\frac{dP}{dz} \quad (5)$$

(e.g., deMarsily, 1986), where K_ϕ is the intrinsic permeability, and η is the fluid viscosity ($\sim 10^{-4}$ Pa·s for H_2O at 500–600 °C and 200 MPa: Bickle and McKenzie, 1987). Fluid-pressure gradients of -1500 to -19000 Pa/m have been suggested for crustal fluid flow (e.g., Norton and Taylor, 1979; Walther and Orville, 1982). For this range of fluid-pressure gradients, estimated intrinsic permeabilities are 10^{-17}–10^{-21} m^2 for channel 2 (Table 2). These estimates are within the range of laboratory measurements of in-situ permeabilities of Brace (1980) for carbonates and metamorphic rocks (10^{-15}–10^{-21} m^2), and are similar to those proposed for other contact and regional metamorphic terrains where fluid infiltration has occurred ($\sim 10^{-16}$–10^{-21} m^2: e.g., Bickle and Baker, 1990; Baumgartner and Ferry, 1991; Dipple and Ferry, 1992; Léger and Ferry, 1993; Davis and Ferry, 1993; Cartwright and Weaver, 1993; Cartwright and Oliver, unpublished manuscript).

Discussion

The two-dimensional pattern of fluid flow in metamorphic rocks is complex, and fluid fluxes are highly variable on the decimeter to meter scale. However, despite the complexity, the two-dimensional pattern of O isotope resetting at Timberu generally conforms to the predictions of the advective-dispersive fluid flow models and yields estimates for time-integrated advective and dispersive fluid fluxes, the timing of fluid-rock interaction, and intrinsic permeabilities that are similar to those calculated for other terrains. One-dimensional sections through this outcrop, however, may not have produced interpretable $\delta^{18}O$ vs. distance profiles.

Fluid flow through the calc-silicate rocks was largely across the lithological layering, with occasional layer-parallel excursions. Since the layering in the Corella calc-silicate rocks is defined by minor differences in the proportions of minerals, rather than by major differences, there may not be major differences in permeability between layers. Fluid flow across layering probably occurred through networks of microfractures (although little direct evidence for this was observed in thin section), and the variability in intrinsic permeabilities possibly reflects variations in fracture density. If fluid flow occurred during contact metamorphism, the flow system records fluids escaping from the upper dike contact, probably aided by buoyancy. The orientation of the fracture networks at Timberu possibly results from rheological differences between the metadolerite dike and the calc-silicate rocks, with strain being accommodated by ductile deformation in the metadolerite and fracturing in the calc-silicate rocks. The width and spacing of fractures required to accommodate the fluid flow is related to intrinsic permeability. For fracture-hosted fluid flow, substituting Equation 5 into Walther and Wood (1984, Eq. 5) produces the following relationship:

$$K_\phi = \frac{a^3 f \tau}{12} \quad (6)$$

where a is the aperture spacing, f is the fracture density (fracture length per squared meter of rock), and τ is tortuosity (~ 0.3–0.7 for metamorphic rocks: Walther and Wood, 1984; Bickle and Baker, 1990). For the range of permeabilities discussed above (10^{-17}–10^{-21} m^2), if microcracks were 10 μm (10^{-5} m) wide, f would equal 2×10^{-5} to 0.24 m/m^2, whereas for 100-μm cracks, f would equal 2×10^{-8} to 2×10^{-4} m/m^2. These calculations indicate that relatively low fracture densities are required to permit fluid fluxes of the magnitude inferred at Timberu. Regardless of the absolute values, inspection of Equations 5 and 6 indicates that, if fluid flow occurred for similar periods throughout the region sampled, the order of magnitude variation in time-integrated fluid fluxes reflects variations in intrinsic permeabilities that may correlate to microfracture density.

Values of D_{eT} are of a similar order of magnitude to those of D_{eL}, suggesting that transverse dispersion occurs

over similar scales to longitudinal dispersion (i.e., decimeters to meters). Because in lithified media porosity is a function of permeability (e.g., Bickle and Baker, 1990), the effective diffusion coefficients would have been higher in the zones with higher permeability; this factor may explain why the scale of transverse dispersive transport from channel 2 is slightly less than that of longitudinal dispersive transport at the front of channel 2. For two-dimensional flow with no significant isotopic fractionation due to reaction, Equation 1 reduces to

$$\phi\left(\frac{\partial C_i}{\partial t}\right) = -\nu\left(\frac{\partial C_i}{\partial z_L}\right) + D_{eL}\left(\frac{\partial^2 C_i}{\partial z_L^2}\right) + D_{eT}\left(\frac{\partial^2 C_i}{\partial z_T^2}\right) \quad (7)$$

where z_L and z_T are distances measured as parallel and normal to the main flow direction, respectively. Given a suitable concentration of data, least-squares techniques could be used to solve for D_{eL}, D_{eT}, and ν from Equation 7, in a similar way to that outlined by Bickle and Baker (1990).

Implications

The results of this study have several implications for modeling metamorphic fluid flow.

One-dimensional fluid flow models. If the pattern of fluid flow in other terrains is similar to that at Timberu, the two-dimensional patterns of isotopic resetting may conform to the advection-dispersion models; however, it may not be possible to interpret readily one-dimensional $\delta^{18}O$ vs. distance profiles that cut obliquely across the channels. Additionally, since there is no single characteristic distance of isotopic resetting, calculation of time-integrated fluid fluxes for any given flow system requires high densities of measurement.

Partially reset isotopic ratios. Rocks that have $\delta^{18}O$ values between those that are unreset and those that are fully reset are difficult to interpret using one-dimensional advection-dispersion transport models. Molecular diffusion coefficients for O in metamorphic fluids are sufficiently low ($\sim 10^{-8}$–10^{-9} m^2/s; Bickle and McKenzie, 1987; Coghlin, 1990) and metamorphic porosities sufficiently small ($<10^{-3}$: Bickle and Baker, 1990) that, on geological time scales, transport by molecular diffusion only occurs over distances of a few centimeters to a few meters (e.g., as documented by Ganor et al., 1989, and Cartwright and Valley, 1991). Hence, in medium to large flow systems (in excess of 10 m) most rocks should be either unreset (ahead of the front) or fully reset (behind the front). Some studies of small-scale one dimensional fluid flow have found O isotope profiles that closely resemble those in Figure 5 (e.g., Bickle and Baker, 1990). However, studies of flow systems on the meter or kilometer scale have found that metasomatic rocks at any given distance along the postulated flow path often have $\delta^{18}O$ values that range between unreset and fully reset (e.g., Nabelek et al., 1992; Ferry and Dipple, 1992; Cartwright and Weaver, 1993). It is highly unlikely that every sample collected several tens or hundreds of meters along a flow path is from part of an isotopic front that is only a few meters wide, and other explanations for partially reset isotopic ratios are required.

Dipple and Ferry (1992) showed that a range of $\delta^{18}O$ values may be produced at any distance along the flow path during polythermal fluid flow, if fluid fluxes are variable. However, polythermal fluid flow may not be ubiquitous, and fluid flow in systems on a scale of meters to tens of meters (e.g., adjacent to large igneous bodies or across layered metamorphic rocks) is probably close to isothermal, making it difficult to use polythermal fluid flow to explain the scatter of isotopic data in these localities. Blattner and Lassey (1989), Bowman and Willett (1991), and Bowman et al. (1994) showed that, if the rate of isotopic equilibration between the rock and the infiltrating fluid is relatively slow, broad sigmoidal fronts may be produced during fluid infiltration. However, although isotopic disequilibrium may be significant at low temperatures, calculations of the rate of isotopic equilibrium in metamorphic rocks (e.g., Bickle and Baker, 1990; Bowman et al., 1994; Dipple and Ferry, 1992) suggest that local isotopic equilibrium is approached at elevated temperatures (>500 °C). Kinematic dispersion may be important in some flow systems, especially where fluid flux rates are high (Bear, 1972). Significant kinematic dispersion also results in broad isotopic fronts, and Bowman et al. (1994) proposed that kinematic dispersion was an important process during relatively rapid fluid flow around the Alta stock, Utah.

The results of this study show that partially reset O isotope ratios may also result from transverse dispersion during channeled isothermal fluid flow. Indeed, depending on the width and spacing of the channels, the volume of partially reset rocks at any outcrop may be much larger than those that are either fully reset or unreset, and, if the channeling persists along the flow path, partially reset rocks may be found at all distances from the geochemical discontinuity. Hence, partially reset isotopic ratios by themselves do not indicate the operation of polythermal fluid flow or isotopic disequilibrium. Although polythermal fluid flow and isotopic disequilibrium apply to certain geological situations, either well-defined isotopic profiles or other evidence, for example, petrological data that indicate polythermal fluid flow (e.g., Baumgartner and Ferry, 1991; Ferry, 1991; Ferry and Dipple, 1992; Cartwright and Oliver, 1992) or discordant O isotope fractionations that suggest isotopic disequilibrium, is required to confirm the operation of these processes.

Decoupling of geochemical parameters. Transverse dispersion may explain discrepancies among the fluid fluxes calculated from different geochemical parameters. For example, the transport of Sr and O isotopes in the Trois Seigneurs Massif, France, appears to have been decoupled during metasomatism (Bickle and Chapman, 1990; Bickle, 1992). Equation 3 shows that dispersive transport distances for a chemical component are inversely proportional to the rock-fluid partition coefficient. Since flu-

id-rock partition coefficients for Sr are much lower than for O (Bickle and McKenzie, 1987), transverse dispersion may homogenize O isotope ratios on the meter scale but not Sr isotope ratios. Similar decoupling between H, O, and C isotope ratios is also likely.

Acknowledgments

Discussions with I.S. Buick, G.M. Dipple, N.H.S. Oliver, T.R. Weaver, and J.K. Vry helped to formulate some of the ideas presented here. J.B. Brady and J.R. Bowman are thanked for helpful and courteous reviews. I.C. acknowledges receipt of ARC grants A39030662 and A39231141 and an ARC Queen Elizabeth II fellowship. D. Gelt drafted Figs. 1 and 2a. This paper is a contribution to IGCP Project 304: Lower Crustal Processes.

References cited

Baumgartner, L.P., and Ferry, J.M. (1991) A model for coupled fluid-flow and mixed-volatile mineral reactions with applications to regional metamorphism. Contributions to Mineralogy and Petrology, 106, 273–285.

Bear, J. (1972) Dynamics of fluid in porous media, 764 p. Dover, New York.

Bickle, M.J. (1992) Transport mechanisms by fluid-flow in metamorphic rocks: Oxygen and strontium decoupling in the Trois Seigneurs Massif: A consequence of kinetic dispersion? American Journal of Science, 292, 289–316.

Bickle, M.J., and Baker, J. (1990) Advective-diffusive transport of isotopic fronts: An example from Naxos, Greece. Earth and Planetary Science Letters, 97, 78–93.

Bickle, M.J., and Chapman, H.J. (1990) Strontium and oxygen isotope decoupling in the Hercynian Trois Seigneurs Massif, Pyrennes: Evidence for fluid circulation in a brittle regime. Contributions to Mineralogy and Petrology, 104, 332–347.

Bickle, M.J., and McKenzie, D.M. (1987) The transport of heat and matter by fluids during metamorphism. Contributions to Mineralogy and Petrology, 95, 384–392.

Blattner, P., and Lassey, K.R. (1989) Stable isotope exchange fronts, Damköhler numbers, and fluid to rock ratios. Chemical Geology, 78, 381–392.

Bowman, J.R., and Willett, S.D. (1991) Spatial patterns of oxygen isotope exchange during one-dimensional fluid infiltration. Geophysical Research Letters, 18, 971–974.

Bowman, J.R., Willett, S.D., and Cook, S.J. (1994) One-dimensional models of oxygen isotopic transport and exchange during fluid flow: Constraints from spatial patterns of oxygen isotopic compositions on fluid fluxes and flow parameters. American Journal of Science, in press.

Brace, W.F. (1980) Permeability of crystalline and argillaceous rocks. International Journal of Rock Mechanics and Mineral Science, 17, 241–251.

Cartwright, I., and Oliver, N.H.S. (1992) The direction of fluid flow during contact metamorphism in the Burstall granite contact aureole. Journal of the Geological Society, London, 149, 693–696.

Cartwright, I., and Valley, J.W. (1991) Steep oxygen-isotope gradients at marble-metagranite contacts in the northwest Adirondack Mountains, New York, USA: Products of fluid-hosted diffusion. Earth and Planetary Science Letters, 107, 148–163.

Cartwright, I., and Weaver, T.R. (1993) Metamorphic fluid flow at Stephen Cross Quarry, Quebec: Stable isotopic and petrological data. Contributions to Mineralogy and Petrology, 113, 533–544.

Clayton, R.N., and Mayeda, T.K. (1963) The use of bromine pentafluoride in the extraction of oxygen from oxides and silicates for isotopic analysis. Geochimica et Cosmochimica Acta, 27, 43–52.

Coghlin, R.A.N. (1990) Studies in diffusional transport: Grain boundary transport of oxygen in feldspars, diffusion of oxygen, strontium and the REEs in garnet, and thermal histories of granitic intrusions in south-central Maine using oxygen isotopes. Ph.D. thesis, Brown University, Providence, Rhode Island.

Cole, D.R., and Ohmoto, H. (1986) Kinetics of isotopic exchange at elevated temperatures and pressures. Mineralogical Society of America Reviews in Mineralogy, 16, 41–90.

Crank, J. (1975) The mathematics of diffusion, 414 p. Oxford University Press, Oxford, England.

Davis, S.R., and Ferry, J.M. (1993) Fluid infiltration during contact metamorphism of interbedded marble and calc-silicate hornfels, Twin Lakes area, central Sierra Nevada, California. Journal of Metamorphic Geology, 11, 71–88.

deMarsily, G. (1986) Quantitative hydrogeology, 440 p. Academic, San Diego, California.

Dipple, G.M., and Ferry, J.M. (1992) Fluid flow and stable isotopic alteration in rocks at elevated temperatures with applications to metamorphism. Geochimica et Cosmochimica Acta, 56, 3539–3550.

Etheridge, M.A., Wall, V.J., and Vernon, R.H. (1983) The role of the fluid phase during regional metamorphism and deformation. Journal of Metamorphic Geology, 1, 205–226.

Ferry, J.M. (1991) Dehydration and decarbonation reactions as a record of fluid infiltration. Mineralogical Society of America Reviews in Mineralogy, 26, 351–393.

Ferry, J.M., and Dipple, G.M. (1992) Models for coupled fluid flow, mineral reaction, and isotopic alteration during contact metamorphism: The Notch Peak aureole, Utah. American Mineralogist, 77, 577–591.

Ganor, J., Matthews, A., and Paldor, N. (1989) Constraints on effective diffusivity during oxygen isotope exchange at a marble-schist contact, Sifnos (Cyclades), Greece. Earth and Planetary Science Letters, 94, 208–216.

Harris, N.W.B., and Bickle, M.J. (1989) Advective fluid transport during charnockite formation: An example from southern India. Earth and Planetary Science Letters, 93, 151–156.

Holcombe, R.J., Pearson, P.J., and Oliver, N.H.S. (1991) Geometry of a Middle Proterozoic extensional décollement in northeastern Australia. Tectonophysics, 191, 255–274.

Labotka, T.C., Nabelek, P.I., and Papike, J.J. (1988) Fluid infiltration through the Big Horse Limestone member in the Notch Peak aureole, Utah. American Mineralogist, 73, 1302–1324.

Léger, A., and Ferry, J.M. (1993) Fluid infiltration and regional metamorphism of the Waits River Formation, north-east Vermont, USA. Journal of Metamorphic Geology, 11, 3–30.

McCrea, J.M. (1950) On the isotope chemistry of carbonates and a paleotemperature scale. Journal of Chemical Physics, 18, 849–857.

Nabelek, P.I., Labotka, T.C., and Russ-Nabelek, C. (1992) Stable isotope evidence for the role of diffusion, infiltration, and local structure on contact metamorphism of calc-silicate rocks at Notch Peak, Utah. Journal of Petrology, 33, 557–583.

Norton, D., and Taylor, H.P. (1979) Quantitative simulation of the hydrothermal systems of crystallizing magmas on the basis of transport theory and oxygen isotope data: An analysis of the Skaergaard intrusion. Journal of Petrology, 20, 421–486.

Oliver, N.H.S., Valenta, R.K., and Wall, V.J. (1990) The effect of heterogeneous stress and strain on metamorphic fluid flow, Mary Kathleen, Australia, and a model for large-scale fluid circulation. Journal of Metamorphic Geology, 8, 311–331.

Oliver, N.H.S., Holcombe, R.J., Hill, E.J., and Pearson, P.J. (1991) Tectono-metamorphic evolution of the Mary Kathleen Fold Belt, northwest Queensland: A reflection of mantle plume processes? Australian Journal of Earth Sciences, 38, 425–455.

Oliver, N.H.S., Wall, V.J., and Cartwright, I. (1992) Internal control of fluid compositions in amphibolite-facies scapolitic calc-silicates, Mary Kathleen, Australia. Contributions to Mineralogy and Petrology, 111, 94–112.

Page, R.W. (1978) Response of U-Pb zircon and Rb-Sr total-rock and mineral systems to low-grade regional metamorphism in Proterozoic igneous rocks, Mount Isa, Australia. Journal of the Geological Society of Australia, 25, 141–164.

——— (1983a) Chronology of magmatism, skarn formation and uranium mineralisation, Mary Kathleen, Queensland, Australia. Economic Geology, 78, 838–853.

——— (1983b) Timing of superposed volcanism in the Proterozoic Mt. Isa Inlier, Australia. Precambrian Research, 21, 223–245.

Rumble, D., and Spear, F.S. (1983) Oxygen-isotope equilibration and permeability enhancement during regional metamorphism. Journal of the Geological Society, London, 140, 619–628.

Valley, J.W. (1986) Stable isotope geochemistry of metamorphic rocks. Mineralogical Society of America Reviews in Mineralogy, 16, 445–490.

Walther, J.V., and Orville, P.M. (1982) Volatile production and transport in regional metamorphism. Contributions to Mineralogy and Petrology, 79, 252–257.

Walther, J.V., and Wood, B.J. (1984) Rate and mechanism in prograde metamorphism. Contributions to Mineralogy and Petrology, 88, 246–259.

Wood, B.J., and Walther, J.V. (1986) Fluid flow during metamorphism and its implications for fluid-rock ratios. In J.V. Walther, and B.J. Wood, Eds. Fluid-rock interactions during metamorphism: Advances in geochemistry, vol. 6, p. 89–108. Springer-Verlag, New York.

Yardley, B.W.D., and Lloyd, G.E. (1989) An application of cathodoluminescence microscopy to the study of textures and reactions in high-grade marbles from Connemara, Ireland. Geological Magazine, 126, 333–337.

Manuscript received February 11, 1993
Manuscript accepted December 31, 1993